Received: 29 January 2021 | Revised: 22 September 2021 | Accepted: 25 September 2021

DOI: 10.1111/pce.14200

ORIGINAL ARTICLE

Plant, Cell & Environment WILEY

ZRT-IRT-Like PROTEIN 6 expression perturbs local ion homeostasis in flowers and leads to anther indehiscence and male sterility

Julien Spielmann[1] | Nathalie Detry[2] | Noémie Thiébaut[1] | Alice Jadoul[1] | Marie Schloesser[1] | Patrick Motte[1] | Claire Périlleux[2] | Marc Hanikenne[1]

[1]InBioS-PhytoSystems, Functional Genomics and Plant Molecular Imaging, University of Liège, Liège, Belgium

[2]InBioS-PhytoSystems, Laboratory of Plant Physiology, University of Liège, Liège, Belgium

Correspondence
Marc Hanikenne, InBioS – PhytoSystems, University of Liège, Quartier de la Vallée, 1, Chemin de la Vallée, 4 - Bât B22, B4000 Liège, Belgium.
Email: marc.hanikenne@uliege.be

Present address
Julien Spielmann, Plant Science Research Laboratory (LRSV), UMR5546 CNRS/ University of Toulouse 3, 31320, Auzeville-Tolosane, France

Funding information
Belgian Federal Science Policy Office, Grant/Award Number: IAP no. P7/44; Fonds De La Recherche Scientifique - FNRS, Grant/Award Numbers: PDR-T.0206.13, MIS-F.4511.16, CDR J.0009.17, PDR T0120.18; Université de Liège, Grant/Award Number: SFRD-12/03

Abstract

Metallic micronutrients are essential throughout the plant life cycle. Maintaining metal homeostasis in plant tissues requires a highly complex and finely tuned network controlling metal uptake, transport, distribution and storage. Zinc and cadmium hyperaccumulation, such as observed in the model plant *Arabidopsis halleri*, represents an extreme evolution of this network. Here, non-ectopic overexpression of the *A. halleri ZIP6* (*AhZIP6*) gene, encoding a zinc and cadmium influx transporter, in *Arabidopsis thaliana* enabled examining the importance of zinc for flower development and reproduction. We show that *AhZIP6* expression in flowers leads to male sterility resulting from anther indehiscence in a dose-dependent manner. The sterility phenotype is associated to delayed tapetum degradation and endothecium collapse, as well as increased magnesium and potassium accumulation and higher expression of the *MHX* gene in stamens. It is rescued by the co-expression of the zinc efflux transporter AhHMA4, linking the sterility phenotype to zinc homeostasis. Altogether, our results confirm that *AhZIP6* is able to transport zinc *in planta* and highlight the importance of fine-tuning zinc homeostasis in reproductive organs. The study illustrates how the characterization of metal hyperaccumulation mechanisms can reveal key nodes and processes in the metal homeostasis network.

KEYWORDS
anther indehiscence, endothecium, magnesium, male sterility, pollen, potassium, tapetum, zinc

1 | INTRODUCTION

Plants need nutrients such as metal ions for their growth and development and, therefore, absorb and distribute those nutrients in adequate concentrations to all organs and cell types. For this purpose, plants possess a complex homeostatic network composed of transcriptional regulators, transmembrane transporters and chelating molecules enabling the uptake and movement of metal ions from roots to seeds (Hanikenne, Esteves, Fanara, & Rouached, 2021; Olsen & Palmgren, 2014; Ricachenevsky, Menguer, Sperotto, & Fett, 2015; Sinclair & Krämer, 2012; Spielmann & Vert, 2021). Metal availability is critical for plant reproduction, since reproductive tissues are highly active and fast-growing tissues, with a high requirement for metals acting mainly as co-factors (Walker & Waters, 2011). This was shown by transcriptomic and proteomic analyses during male gametophyte development within stamens, which revealed that more than 300 metal-related genes are expressed in this organ including numerous metal transporters and zinc-finger proteins (Walker & Waters, 2011). Consistently, mutations leading to perturbations of iron, copper or zinc homeostasis often cause sterility. For instance, ferritin-defective *Arabidopsis thaliana* mutants display impaired flower development and seed formation (Ravet et al., 2009). Loss of function

of transcription factors controlling copper homeostasis (SPL7 and CITF1) impairs anther dehiscence, pollen abundance and viability (Yan et al., 2017). The *frd3*, *opt3* or *ysl1ysl3 A. thaliana* mutants, defective in metal and/or metal chelator transporters, suffer from pollen viability defect or arrested embryo development (Roschzttardtz, Seguela-Arnaud, Briat, Vert, & Curie, 2011; Stacey et al., 2008; Stacey, Koh, Becker, & Stacey, 2002; Waters et al., 2006). Similarly, a *hma2 hma4* double mutant that is unable to efficiently transfer zinc from roots to shoots, is also male sterile due to pollen defect (Hussain et al., 2004). Thus, a finely tuned metal homeostasis is key to ensure a successful reproduction as well as seed yield and nutritive quality.

During evolution, plants colonized a large variety of environments that substantially differ in metal availability. An extreme case is represented by a small number of plant species (around 720) that have developed a so-called hyperaccumulation strategy and colonize soils heavily polluted by metals (Hanikenne & Nouet, 2011; Krämer, 2010; Merlot, de la Torre, & Hanikenne, 2021; Reeves et al., 2018; van der Ent, Baker, Reeves, Pollard, & Schat, 2013). Hyperaccumulator plants are highly metal tolerant and actively absorb, efficiently transport and accumulate metals in shoot tissues (e.g., >3,000 $\mu g.g^{-1}$ of zinc in leaf dry weight) (Krämer, 2010), without toxicity symptoms. Most of these plants are nickel hyperaccumulators whereas only a few are zinc and cadmium hyperaccumulators, such as the model species *Arabidopsis halleri* (Hanikenne & Nouet, 2011; Krämer, 2010; Merlot et al., 2021; van der Ent et al., 2013). About 30 candidate genes were identified for a role in metal hyperaccumulation and hypertolerance in *A. halleri* (Krämer, Talke, & Hanikenne, 2007; Merlot et al., 2021; Talke, Hanikenne, & Krämer, 2006). Among those, *ZIP6* (*ZRT-IRT-Like PROTEIN 6*) encodes a zinc and cadmium transporter of the ZIP (ZINC-REGULATED-, IRON-REGULATED-LIKE TRANSPORTER PROTEIN) family, and is one of the few genes whose function has been experimentally examined by gene silencing in *A. halleri* (Spielmann et al., 2020), together with *HMA4* (*HEAVY METAL ATPASE 4*), *NAS2* (*NICOTIANAMINE SYNTHASE 2*) and *CAX1* (*CATION EXCHANGER 1*) (Ahmadi, Corso, Weber, Verbruggen, & Clemens, 2018; Deinlein et al., 2012; Hanikenne et al., 2008). The *ZIP6* gene is duplicated in the *A. halleri* genome and both copies are constitutively overexpressed in *A. halleri* compared to *A. thaliana*. With highly similar coding sequences, but very divergent promoters, the two *A. halleri ZIP6* copies (*AhZIP6-1* and *AhZIP6-2*) display partly organ-specific roles in roots and aerial parts, and differentially impact metal homeostasis and tolerance in the plant (Spielmann et al., 2020).

Here, we extended the characterization of the AhZIP6 transporter to its role in flower development and fertility. We showed that in *A. thaliana*, the expression level of *AhZIP6-1* positively correlated with a male sterility phenotype resulting from anther indehiscence. Characterization of this phenotype revealed a local perturbation of cation (magnesium and potassium) homeostasis in stamens of *AhZIP6-1* plants. Complementation of male sterility upon co-expression of *AhZIP6-1* and *AhHMA4* genetically linked this phenotype to altered zinc homeostasis. These observations confirmed that ZIP6 is able to transport zinc *in planta* and highlighted that fine-tuning of the zinc homeostasis network is required for fertility and reproduction in plants.

2 | RESULTS

2.1 | Expression of *AhZIP6* causes sterility in *A. thaliana*

We used *A. thaliana* T3 homozygous transgenic lines expressing *AhZIP6* under the control of either pAhZIP6-1 (*AhZIP6-1* lines) or pAhZIP6-2 (*AhZIP6-2* lines) promoters (Spielmann et al., 2020) to examine the impact of *AhZIP6* expression on reproduction. *AhZIP6-1* homozygous lines harbored smaller siliques (∼0.4 cm in length) than wild-type Col-0 plants (∼1.4 cm in length). These small siliques were unfertilized carpels and no seeds were produced compared to an average of 51 seeds per silique in Col-0 (Figure 1a,b). In contrast, heterozygous *AhZIP6-1* and homozygous *AhZIP6-2* plants produced normal siliques and seeds (Figure 1a,b). To identify whether the lack of fertilization in *AhZIP6-1* homozygous lines was due to male and/or female defects, manual fertilization and reciprocal crossings were performed. Application of pollen from wild-type or homozygous *AhZIP6-1* plants on stigmata of homozygous *AhZIP6-1* plants partially rescued the phenotype since 1.36 and 1.01 cm long siliques containing an average of 32 and 18 seeds were produced, respectively (Figure 1a,b). The partial complementation potentially resulted from the difficulty to apply enough pollen on the stigmata during hand crossing. These observations indicated that both female and male gametophytes of *AhZIP6-1* plants were functional. Pollen germination assays, as well as lugol and Alexander staining, further confirmed that pollen grains were viable (Figure S1). Moreover, self-fertilization of heterozygous *AhZIP6-1* plants or manual crossing between heterozygous and homozygous *AhZIP6-1* plants showed Mendelian segregation of the phenotype and confirmed that male and female gamete fertility were unaltered in *AhZIP6-1* lines (Table 1a,b).

2.2 | Sterility is determined by the inflorescence genotype

Grafting experiments were next performed to determine which part of the plant among roots, shoot and inflorescence was responsible for the observed phenotype. First, grafting shoots of homozygous *AhZIP6-1* plants on Col-0 roots did not rescue the silique phenotype, whereas the plants obtained with the reciprocal grafting had no phenotype (Figure 2a), indicating a shoot-dependent phenotype. Second, floral stem grafting was performed. Homozygous *AhZIP6-1* floral stems grafted on Col-0 plants developed short siliques (∼0.42 cm in length), although the inflorescences formed on the axillary branches of the Col-0 rosettes developed 'normal' siliques (∼0.91 cm in length). Reciprocally, Col-0 floral stems grafted on homozygous *AhZIP6-1* plants developed normal siliques (∼0.96 cm in length) and axillary floral stems formed in the *AhZIP6-1* rosettes displayed unfertilized carpels (∼0.4 cm in length) (Figure 2b). Note that in all grafting experiments, fertilized siliques were smaller than in un-grafted controls, probably because of the stressful procedure. Taken together, these experiments indicated that the sterility phenotype was due to a local perturbation in *AhZIP6-1* flowers.

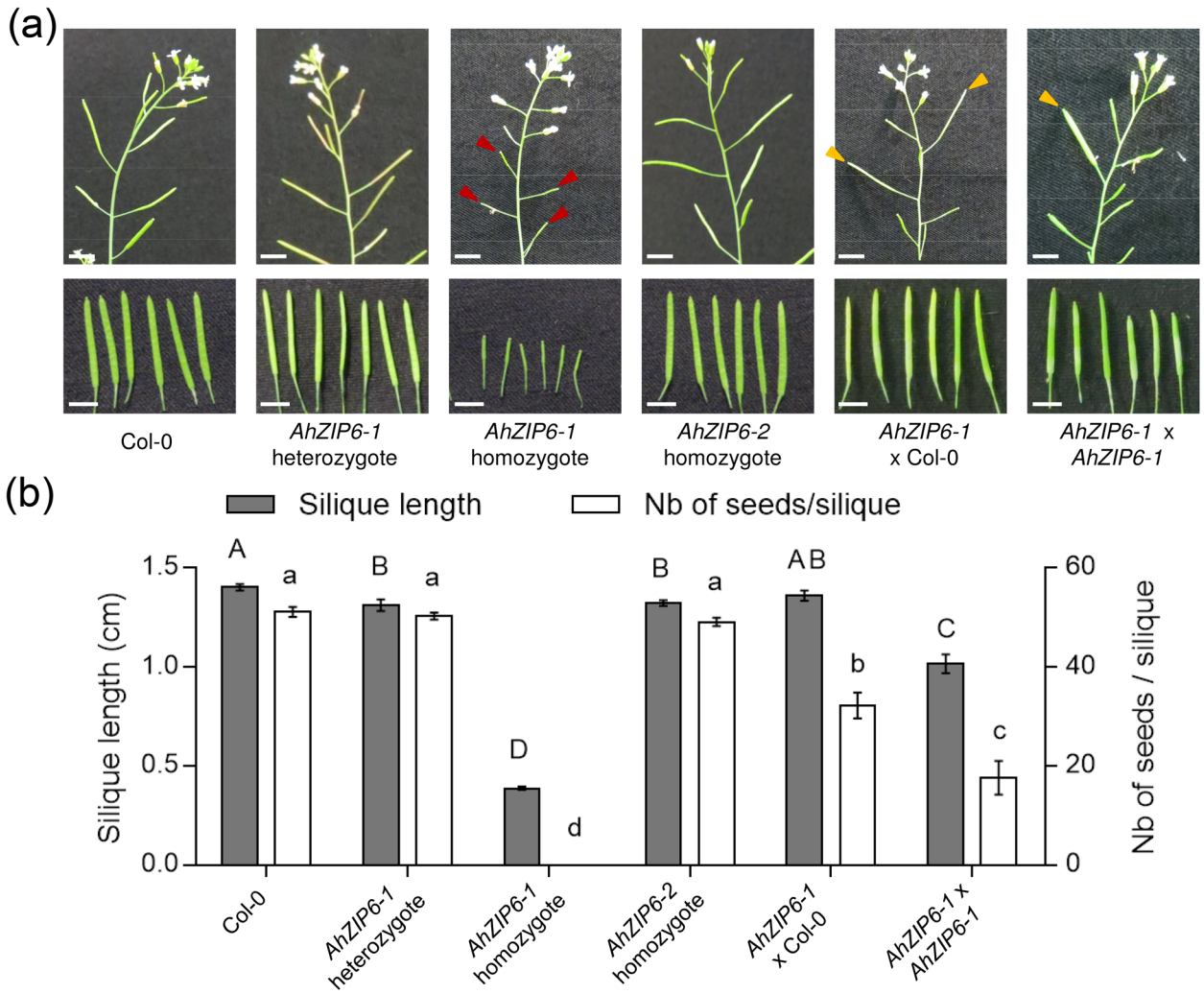

FIGURE 1 Silique length and number of seeds per silique in *A. thaliana* expressing *AhZIP6*. (a) Pictures of inflorescence (top) or silique (bottom) and (b) silique length and number of seeds per silique in different genotypes of *A. thaliana* and after different crosses. The mother plants for crosses (x) always had a homozygote pAhZIP6-1::*AhZIP6* genotype. Red and orange arrowheads point to short and complemented siliques, respectively. Values (means ± SEM; from one experiment representative of two independent experiments, with for self-pollination, 20 siliques for three independent lines per genotype and, for crosses, 6–19 siliques from successful crosses). Data were analysed by one-way ANOVA followed by Tukey multiple comparison post-test. Statistically significant differences between means are indicated by letters ($p < .05$). Scale bars: 5 mm [Colour figure can be viewed at wileyonlinelibrary.com]

2.3 | Sterility correlates with *ZIP6* expression level in flowers

Two observations suggested that *ZIP6* gene dosage in flowers may be key to determine the sterility phenotype. First, the sterility phenotype was only observed in homozygous *AhZIP6-1* plants and not in the heterozygous lines (Figure 1). Second, we have shown that *AhZIP6-1* and *AhZIP6-2* have distinct expression patterns, with *AhZIP6-1* and *AhZIP6-2* being predominantly expressed in shoots and roots, respectively (Spielmann et al., 2020). To determine if sterility in *AhZIP6-1* plants was a consequence of local differences in *ZIP6* expression level in flowers, silique size (as a proxy for sterility) and *AtZIP6* and *AhZIP6* expression levels were scored simultaneously in individual plants of different genotypes: Col-0, homozygous *AhZIP6-1* or *AhZIP6-2* plants and heterozygous *AhZIP6-1* plants. In our growth conditions, 22.3% of Col-0 siliques were found to be short and/or unfertilized (Figure 3a) while this proportion was 96.8% in *AhZIP6-1* homozygous plants. Heterozygous *AhZIP6-1* and homozygous *AhZIP6-2* plants displayed an intermediate phenotype with 39.8% and 26.3% of unfertilized siliques, respectively, which was not significantly different from Col-0 (Figure 3a). Regarding the expression level of *AhZIP6-1*, it was 10-fold higher than *AtZIP6* in Col-0, *AhZIP6-1* or *AhZIP6-2* plants and two-fold higher in homozygous *AhZIP6-1* than in heterozygous *AhZIP6-1* or homozygous *AhZIP6-2* plants (Figure 3b). Sterility and total *ZIP6* expression level (*AtZIP6* + *AhZIP6*) in inflorescences of *AhZIP6-1* and *AhZIP6-2* plants were positively correlated (Figure 3c) suggesting that the sterility phenotype was a direct consequence of *ZIP6* expression.

2.4 | Male sterility results from anther indehiscence

Detailed observation of stamens of homozygous *AhZIP6-1* plants revealed that pollen was not properly released due to anther dehiscence failure (Figure 4a). Cross sections were performed at flower development stages 9, 11 and 13 [according to Sanders et al., 1999]. As expected, in wild-type and *AhZIP6-2* anthers, tapetum degeneration occurred between stages 9 and 11, whereas in the *AhZIP6-1* lines, tapetum was still present at stage 11 indicating a delay in tapetum degeneration (Figure 4b and Figure S2). Moreover, endothecium thickening and lignification were not observed in the *AhZIP6-1* anthers in contrary to wild-type and *AhZIP6-2* anthers (Figure 4c).

To link these observations to the local expression pattern of *ZIP6* in the anthers, promoter-GUS reporter lines were analysed. The *AhZIP6-1* promoter (pAhZIP6-1) drove strong GUS expression in the filament and anthers, mainly in the stamen connective tissue (Figure 4d). In contrast, the *AhZIP6-2* promoter (pAhZIP6-2) was barely active in flowers (Figure 4d). Similar patterns were found in *A. halleri*, indicating conserved regulation of the *AhZIP6* copies when heterologously expressed under the control of their native promoter in *A. thaliana* (Figure S3). *ZIP6* transcript quantification in Col-0, *AhZIP6-1* and *AhZIP6-2* plants confirmed that *AhZIP6-1* was strongly expressed in stamens, ~5- and 2-fold higher than *AtZIP6* and *AhZIP6-2*, respectively (Figure 4e). Differences in *AhZIP6-1* and *AhZIP6-2* expression levels were observed in inflorescences, flowers and stamens (Figures 3b and 4e). However, relative *AhZIP6-1* expression was two-fold higher in stamens than in flowers or inflorescences, confirming the localized perturbation (Figures 3b and 4e).

TABLE 1 Analysis of gamete fertility

(a) Segregation of *AhZIP6-1* heterozygote plant progenies				
	WT (%)	**HT (%)**	**HM (%)**	**Total**
Theoretical	NA	66.6	33.3	$N = 900$
Experimental	NA	68.8	31.2	
(b) Segregation of a cross between plants homozygote and heterozygote for *AhZIP6-1*				
	WT (%)	**HT (%)**	**HM (%)**	**Total**
Theoretical	0	50	50	$N = 302$
Experimental	0	49.3	50.7	

Note: Segregation analysis in the progeny of self-pollinated pAhZIP6-1::*AhZIP6* heterozygote *A. thaliana* plants (a) and of hand crosses between pAhZIP6-1::*AhZIP6* heterozygote (HT) and homozygote (HM) *A. thaliana* plants (b). (a) Plants were genotyped by PCR after germination under antibiotic selection. Therefore, no wild-type progeny (WT) was recovered. NA: not applicable. (b) Segregation was scored upon visual observation of the silique phenotype. Data were obtained from three independent lines.

2.5 | Magnesium and potassium concentrations are perturbed in *AhZIP6-1* stamens

As AhZIP6 is a zinc transporter (Spielmann et al., 2020), we next assessed whether a change in zinc supply could complement the male sterility phenotype of the *AhZIP6-1* plants. Col-0, *AhZIP6-1* and *AhZIP6-2* plants were therefore grown in hydroponics and, after 3 weeks in control conditions (1 μM Zn), were exposed to zinc deficiency (0 μM Zn) or zinc excess (10 and 20 μM) until silique formation (around 5 weeks). No effect of zinc supply on the phenotype of *AhZIP6-1* lines was observed (Figure S4A).

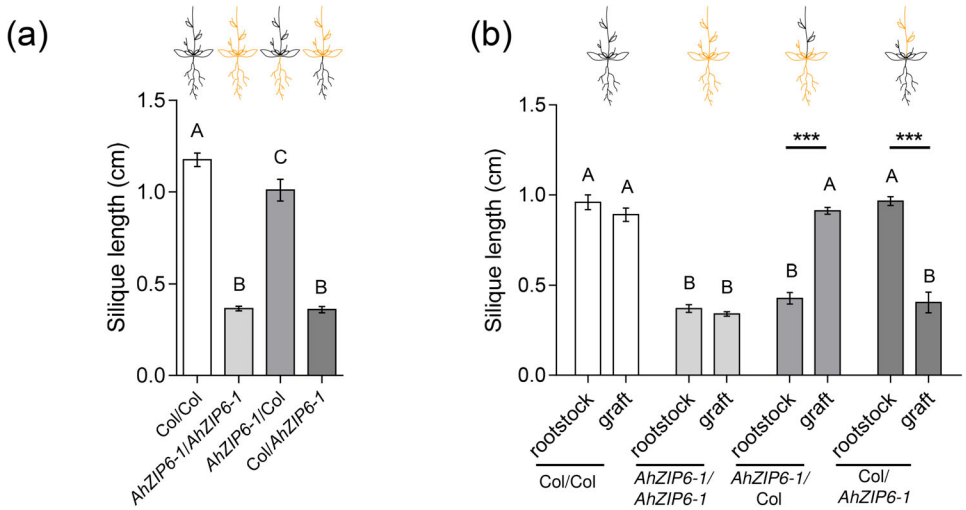

FIGURE 2 Reciprocal grafting of Col-0 and pAhZIP6-1::*AhZIP6* root and floral stems. Silique length of plants after root (a) and floral stem (b) grafting between homozygous plants expressing pAhZIP6-1::*AhZIP6* (in orange) and Col-0 (in black). Values are means ± SEM of 5–7 (a) or 5–11 (b) independently grafted plants per genotype, with a minimum of 10 siliques per plant, respectively. Data were analysed by one-way ANOVA followed by Tukey multiple comparison post-test (a) or by two-way ANOVA followed by Bonferroni multiple comparison post-test (b). Statistically significant differences between means are indicated by letters ($p < .05$) or by asteriks (***$p < .001$) [Colour figure can be viewed at wileyonlinelibrary.com]

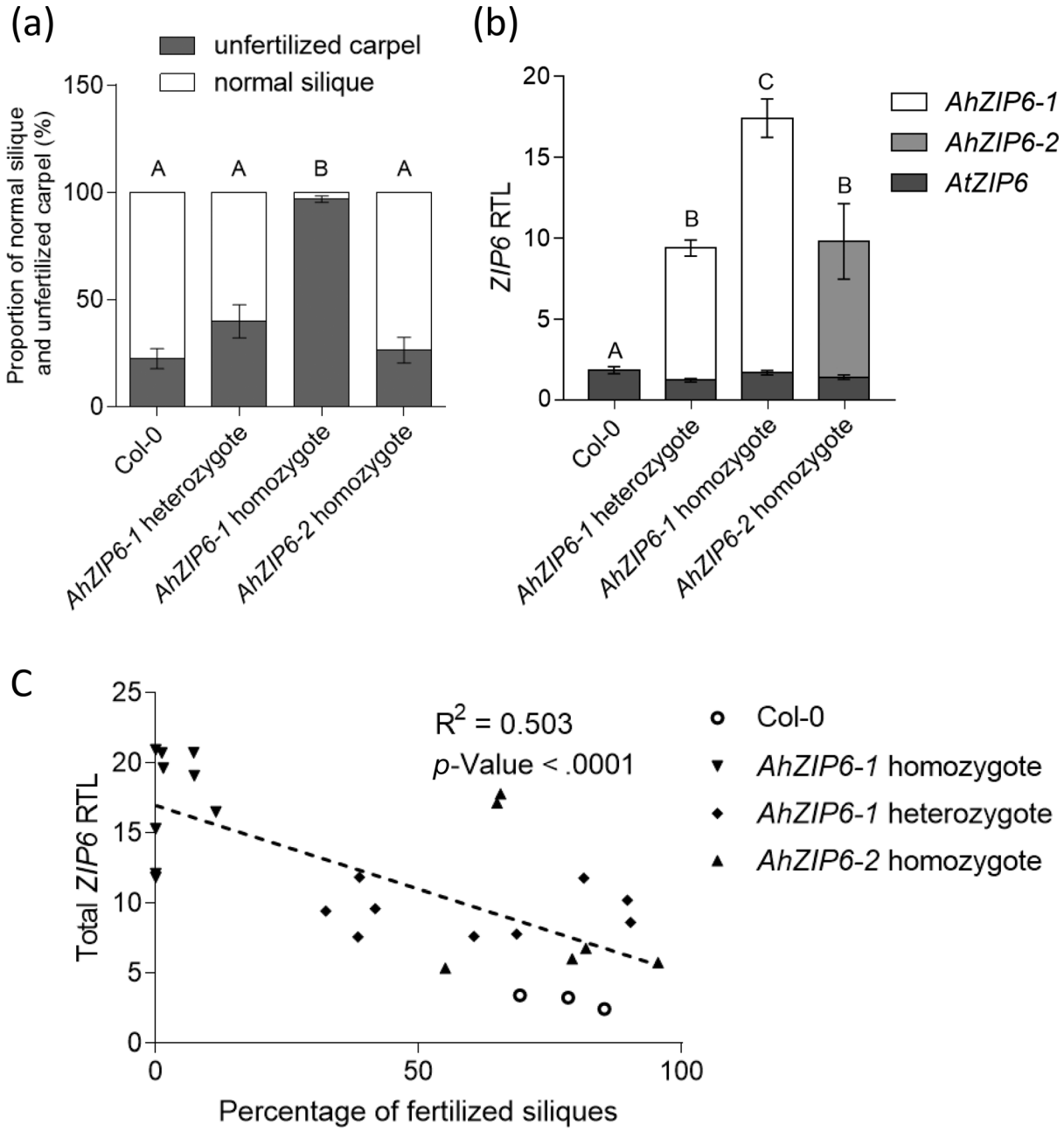

FIGURE 3 Relationship between *ZIP6* expression and fertility. (a) Determination of the proportion of unfertilized carpels of transgenic *A. thaliana* plants expressing pAhZIP6-1::*AhZIP6* (*AhZIP6-1*), pAhZIP6-2::*AhZIP6* (*AhZIP6-2*) or in Col-0 (*AtZIP6*) grown on soil (long days). Values (means ± SEM) are from three biological replicates per line and at least 30 siliques per line. (b) Relative transcript levels (RTL) of *ZIP6* (*AtZIP6* + *AhZIP6*) in inflorescence of the same plants. Values (means ± SEM) are from three biological replicates per line for two or three lines per genotype (Spielmann et al., 2020) and are relative to *EF1a* and At1g58050. (a and b) Data were analysed by one-way ANOVA followed by Tukey multiple comparison post-test. Statistically significant differences between means are indicated by letters ($p < .05$). (c) Correlation analysis (Pearson test) of silique length (a) and total *ZIP6* (*AtZIP6* + *AhZIP6*) expression (b). Note that *AtZIP6*, *AhZIP6-1* and *AhZIP6-2* were amplified with specific primers (b, c) and these expression values were summed up in the correlation analysis (c) for *AhZIP6-1* and *AhZIP6-2* lines

To check whether the homeostasis of other ions was affected by *AhZIP6-1* expression, the ionomes (11 elements) of whole flowers and isolated stamens were analysed in plants grown on soil. The expression of either *AhZIP6* copies had no impact on the ionome of whole flowers or on the concentration of zinc in the stamens (Figure 5c). In contrast, an increased accumulation of magnesium (+30%) and potassium (+58%) was observed in the stamens of *AhZIP6-1* lines compared to Col-0 and *AhZIP6-2* lines (Figure 5a,b). A simultaneous depletion of magnesium and potassium in the medium (0 mM instead of 0.75 mM and 1.58 mM respectively) was not able to restore the fertility of *AhZIP6-1*, comforting the hypothesis of a local perturbation (Figure S4B).

AhZIP6 being a divalent cation transporter, we thus tested its ability to transport magnesium and thereby complement the CM66

yeast strain that lacks the two main magnesium transporters (*ALR1* and *ALR2*) (Li, Tutone, Drummond, Gardner, & Luan, 2001). This strain is unable to grow on a standard synthetic medium and we observed that constitutive expression of *AhZIP6* failed to rescue this phenotype, suggesting that AhZIP6 is not able to transport magnesium (Figure 5d).

Finally, to further examine the possible cause of magnesium accumulation in *AhZIP6-1* stamens, we measured the transcript levels of

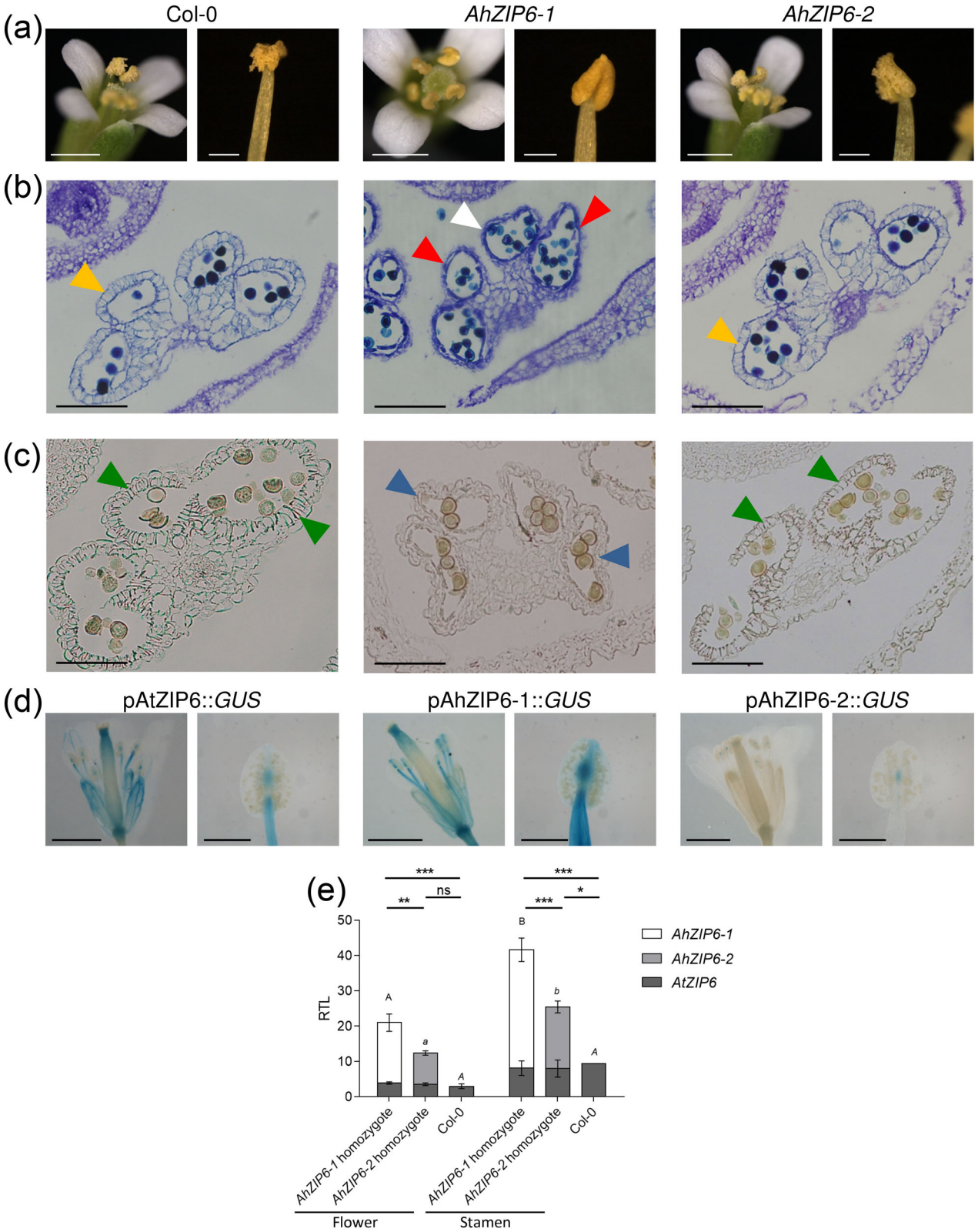

FIGURE 4 Legend on next page.

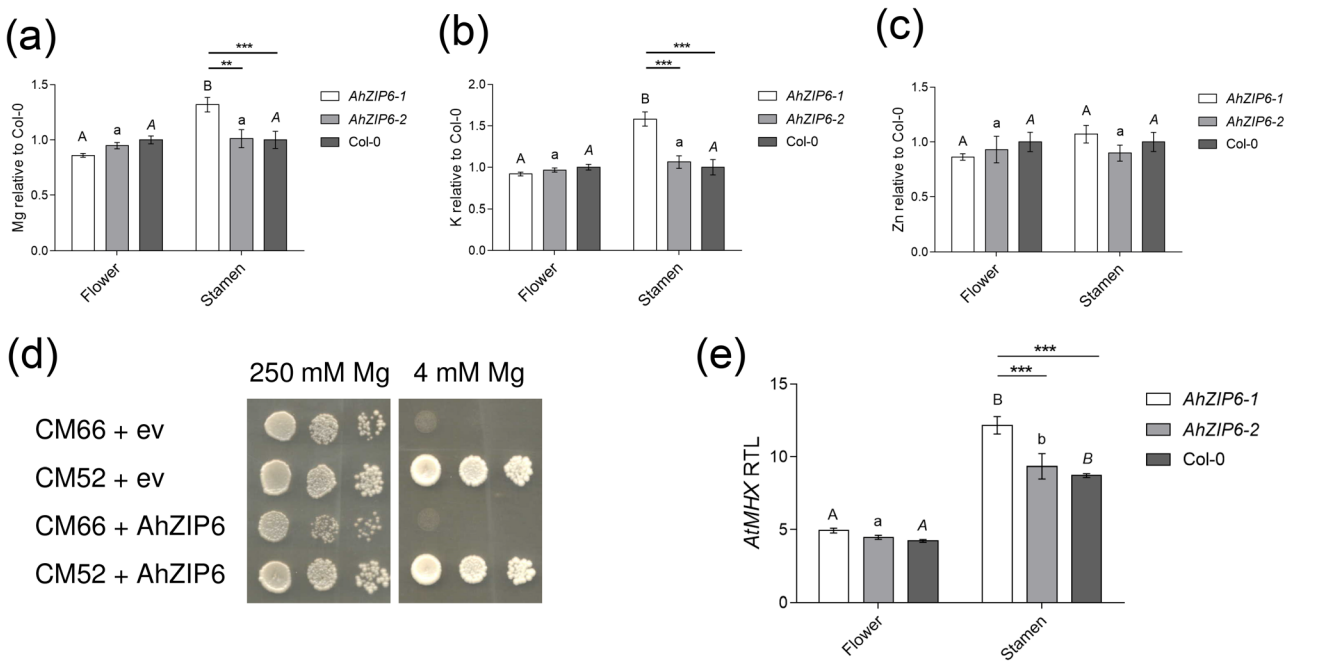

FIGURE 5 Consequences of *AhZIP6* expression on the flower and stamen ionome. (a) Magnesium, (b) potassium and (c) zinc concentrations in flowers and stamens of transgenic homozygous *A. thaliana* plants expressing pAhZIP6-1::*AhZIP6* (*AhZIP6-1*), pAhZIP6-2::*AhZIP6* (*AhZIP6-2*) or in Col-0 plants grown on soil (long days). Values are means ± SEM, with for stamens, three biological replicates each consisting of 100 stamens from three independent lines and for flowers, two biological replicates each consisting of 40 flowers from three independent lines. (d) Expression of *AhZIP6* or the empty vector (ev, pFL38) in the magnesium-sensitive *alr1alr2* double mutant (CM66) and the parental strain CM52. The CM66 strain is unable to grown in control condition (4 mM Mg). Transformants were serially diluted at OD_{600} of 0.2, 0.02, 0.002 (left to right) and spotted on SC-Leu medium with control (4 mM) and excess (250 mM) magnesium concentrations. Pictures were taken after 4 days of incubation at 30°C and are representative of two independent experiments, each including three independent transformants. (e) Relative transcript levels (RTL) of *MHX* in transgenic homozygous *A. thaliana* plants expressing pAhZIP6-1::*AhZIP6* (*AhZIP6-1*), pAhZIP6-2::*AhZIP6* (*AhZIP6-2*) or in Col-0 grown on soil (long days). Values (means ± SEM; for stamens, from two biological replicates each consisting of 800 stamens per genotype, and for flowers: from three biological replicates each consisting of 40 flowers per genotype) are relative to *EF1a* and At1g58050. Data were analysed by two-way ANOVA followed by Bonferroni multiple comparison post-test (a, b, c and e). Statistically significant differences of means between genotypes within a tissue are indicated by asteriks (**p < .01, ***p < .001) and between tissues within a genotype by different letters (p < .05, capital letters: *AhZIP6-1*, lowercase letters: *AhZIP6-2*, capital letters in italic: Col-0) [Colour figure can be viewed at wileyonlinelibrary.com]

the *MHX* gene, which encodes a zinc and magnesium vacuolar transporter that is more abundant in *A. halleri* shoots than in *A. thaliana* (Elbaz et al., 2006). *MHX* transcript levels were around 40% higher in stamens of *AhZIP6-1* lines compared to Col-0 and *AhZIP6-2* lines (Figure 5e). At the whole flower level, no difference in *MHX* expression was found between the three genotypes, which suggested a local effect in stamens (Figure 5e).

2.6 | Expression of AhHMA4 complements the male sterility of AhZIP6-1 lines

As AhZIP6 is hypothesized to mediate zinc (and cadmium) ion influx into the cytoplasm (Spielmann et al., 2020), we next tested the possibility to alter the phenotype of the *AhZIP6-1* plants by overexpressing the *HMA4* gene, encoding a plasma membrane-localized zinc efflux

FIGURE 4 Characterization of anther development in *A. thaliana* expressing *AhZIP6*. (a) Pictures of flowers and stamens (developmental stage 13) of Col-0 and homozygous plants expressing pAhZIP6-1::*AhZIP6* (*AhZIP6-1*) or pAhZIP6-2::*AhZIP6* (*AhZIP6-2*). Cross-section of anthers, stained with Toluidine Blue (developmental stage 11) (b) or, Phloroglucinol (developmental stage 13) (c), in genotypes presented in (a). White, orange, red, green and blue arrows highlight respectively the tapetum, the endothecium secondary thickening, the lack of endothecium secondary thickening and the presence or absence of lignified structure in the endothecium. (d) Histochemical detection of GUS activity (blue) directed by the pAtZIP6, pAhZIP6-1 or pAhZIP6-2 promoters in flowers and stamens. Pictures (a, b, c and d) are representative of six independent lines per construct. (e) Relative transcript levels (RTL) of *ZIP6* (*AtZIP6* + *AhZIP6*) in transgenic homozygous *A. thaliana* plants expressing pAhZIP6-1::*AhZIP6* (*AhZIP6-1*), pAhZIP6-2::*AhZIP6* (*AhZIP6-2*) or in Col-0 (*AtZIP6*) grown on soil (long days). Values (means ± SEM; for stamens, from two biological replicates each consisting of 800 stamens per genotype, and for flowers, from three biological replicates each consisting of 40 flowers per genotype) are relative to *EF1a* and At1g58050. Statistically significant differences of means between genotypes within a tissue are indicated by asteriks (*p < .05, **p < .01, ***p < .001) and between tissues within a genotype by different letters (p < .05, capital letters: *AhZIP6-1*, lowercase italic letters: *AhZIP6-2*, capital letters in italic: Col-0). Scale bars: 1 mm (flower), 200 μm (stamen) and 50 μm (stamen cross-sections) [Colour figure can be viewed at wileyonlinelibrary.com]

transporter. *HMA4* is highly expressed in *A. halleri* and plays a key role in pumping zinc in seeds in *A. thaliana* (Hanikenne et al., 2008; Hussain et al., 2004; Olsen et al., 2016). *AhZIP6-1* plants were crossed with lines expressing *AhHMA4* under the control of the pAhHMA4-2 promoter (Nouet et al., 2015). The F2 plants were sorted in three groups: (a) heterozygote for *AhZIP6* and homozygote for *AhHMA4* (Zo-HH), (b) homozygote for *AhZIP6* and heterozygote for *AhHMA4* (ZZ-Ho) and (c) the double homozygotes (ZZ-HH). These F2 plants as well as control plants (Zo-oo, oo-HH and oo-oo) were then grown on soil and fertility was assessed by visual determination of the silique length. If the expression of *AhHMA4* had no effect on the phenotype, the expectation was that all ZZ plants should be sterile. However, 27.4% of ZZ-Ho plants and the majority (77.6%) of ZZ-HH plants were fertile with normal silique lengths (Figure 6a). This suggested that (a), at the homozygote state, expression of *AhHMA4* in the *AhZIP6-1* background complemented the phenotype, (b) that this complementation was sensitive to *AhHMA4* gene dosage and therefore (c) that the male sterility phenotype possibly resulted from altered zinc allocation. To support these conclusions, the expression pattern of the *GUS* gene under the control of pAhHMA4-2 was determined in flowers. pAhHMA4-2 was active in petal and sepal vascular tissues, in the stigma, in filaments and in the connective of the stamens (Figure 6b). This expression pattern was highly similar to the activity profile of pAhZIP6-1 (Figure 4d) and this co-localization supported the hypothesis that *AhHMA4* expression could locally complement the negative impact of *AhZIP6-1* on male fertility.

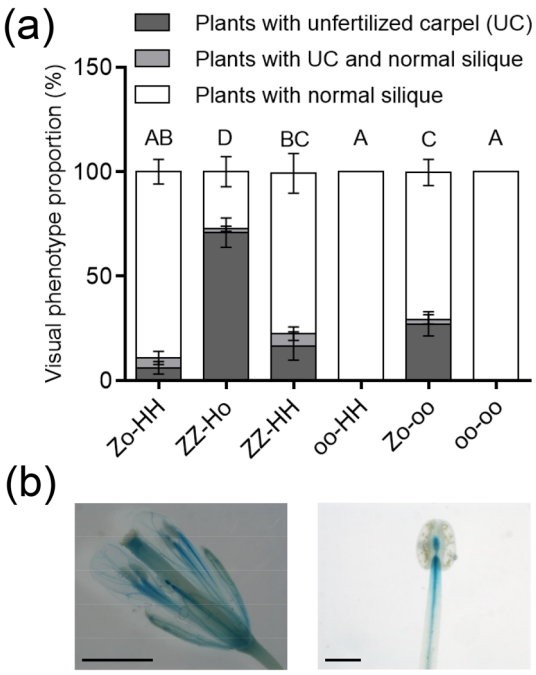

FIGURE 6 Complementation of the male sterility in pAhZIP6-1::*AhZIP6 A. thaliana* plants by pAhHMA4-2::*AhHMA4*. (a) pAhZIP6-1::*AhZIP6* and pAhHMA4-2::*AhHMA4* homozygous plants were crossed and the proportion (%) of plants harboring the sterility phenotype was scored in the F2 progeny (means ± SEM from two independent experiments, each including three to six plants per genotype). The genotype of the plants is indicated as follows: ZZ, homozygote for pAhZIP6-1::*AhZIP6*; Zo, heterozygote for pAhZIP6-1::AhZIP6; HH, homozygote for pAhHMA4-2::*HMA4*; Ho, heterozygote for pAhHMA4-2::*HMA4*; oo: wild-type allele. The phenotype was visually determined by scoring the silique length. Plants with only unfertilized carpels are in dark grey, plants with both unfertilized and normal siliques are in light grey and plants with only normal siliques are in white. Data were analysed by one-way ANOVA comparing the proportion of normal siliques between genotypes followed by Tukey multiple comparison post-test. Statistically significant differences between means are indicated by different letters ($p < .05$). (b) Histochemical detection of GUS activity (blue) directed by the pAhHMA4-2 promoter in flowers and stamens of *A. thaliana*. Scale bars: 1 mm (flower) and 200 μm (stamen) [Colour figure can be viewed at wileyonlinelibrary.com]

3 | DISCUSSION

Zinc is a metal micronutrient with an important, but largely unknown, function in pollen formation or more generally in plant reproduction (Curie et al., 2009; Jochner et al., 2013; Pandey, Pathak, & Sharma, 2006). So far, only few zinc finger proteins have been linked to anther and pollen development (D'Ippolito, Arias, Casalongue, Pagnussat, & Fiol, 2017; Kapoor, Kobayashi, & Takatsuji, 2002; Xu et al., 2020). Here, we showed that expression of *AhZIP6-1*, encoding a zinc and cadmium transporter in *A. halleri* (Spielmann et al., 2020), strongly caused male sterility in *A. thaliana* due to anther indehiscence (Figures 3 and 4). As pollen grains were fully functional (Table 1), anther indehiscence was also responsible for an apparent lower pollen germination in *AhZIP6-1* lines (Figure S1A). We acknowledge that the sterility phenotype observed in the *AhZIP6-1* lines is the result of the cumulative expression of *AtZIP6* and *AhZIP6-1*. However, the contribution of *AtZIP6* to the total *ZIP6* expression is minor (<10%–20%) and ~3-5-fold smaller than the difference of *AhZIP6* expression between *AhZIP6-1* heterozygous (no phenotype) and homozygous (phenotype) lines (Figures 1, 3a,b and 4e).

Anther cross sections revealed that the indehiscence phenotype was linked to two developmental defects in *AhZIP6-1* lines. First, the tapetum degradation was delayed during stamen maturation (Figure 4b and Figure S2). The main function of this cell layer is, upon degradation, to provide nutrients to pollen grains (Gomez, Talle, & Wilson, 2015; Pacini, 2010; Pacini, Franchi, & Hesse, 1985). Most mutations impacting tapetum function lead to pollen development problems (Albrecht, Russinova, Hecht, Baaijens, & de Vries, 2005; Colcombet, Boisson-Dernier, Ros-Palau, Vera, & Schroeder, 2005; Yang et al., 2003; Yang, Vizcay-Barrena, Conner, & Wilson, 2007; Zhu et al., 2008). The expression of *AhZIP6-1* did not impact pollen viability, germination or starch content (Figure S1) suggesting that the main tapetum function was not impacted. However, the degradation of the tapetum cell layer occurred later in *AhZIP6-1* plants compared to Col-0 or *AhZIP6-2* plants (Figure 4b and Figure S2). A delay in tapetum degradation was shown to lead to a delay of dehiscence, suggesting this process to be essential for proper anther opening (Gomez et al., 2015; Kim et al., 2010). We therefore hypothesize that indehiscence of *AhZIP6-1* anthers is, at least in part, a consequence of delayed tapetum degeneration. Second, another point revealed by anther

cross-section observations was a collapsing of the endothecium in *AhZIP6-1* plants due to a lack of lignification of the cell wall of endothecium cells (Figure 4b,c). The endothecium has key functions in procuring forces enabling anther opening (Dawson et al., 1999; Keijzer, 1987; Scott, Spielman, & Dickinson, 2004; Villarreal et al., 2009; Wilson, Song, Taylor, & Yang, 2011). Mutations affecting endothecium development and thickening lead to male sterility phenotypes due to anther indehiscence (Brown, Zeef, Ellis, Goodacre, & Turner, 2005; Jung et al., 2008; Kim, Jung, Jeung, & Shin, 2012; Mitsuda et al., 2007; Mitsuda, Seki, Shinozaki, & Ohme-Takagi, 2005; Steiner-Lange et al., 2003; Yang et al., 2007). The secondary thickening of the endothecium did not occur in *AhZIP6-1* plants, with a collapsing of this cell layer (Figure 4b). Therefore, mechanical forces essential for anther dehiscence were not produced, affecting pollen release by *AhZIP6-1* anthers and leading to sterility.

Anther indehiscence in *AhZIP6-1 A. thaliana* plants was associated with increased potassium and magnesium accumulation in stamens (Figures 4 and 5), possibly accounting for male sterility. Indeed, altered accumulation of potassium, affecting osmotic pressure and water movement, has been linked to altered anther dehiscence (Bassil et al., 2011; Bock et al., 2006; Jakobsen et al., 2005; Matsui, Omasa, & Horie, 2000; Rehman & Yun, 2006; Wei et al., 2018; Wilson et al., 2011). For instance, potassium concentration was shown to increase during anther maturation in barley, with, in particular, accumulation of potassium in the stomium area (Rehman & Yun, 2006) which has a key role in anther dehiscence (Scott et al., 2004). Potassium accumulation in indehiscent *AhZIP6-1* anthers could be seen as an ultimate effort of the plant to force dehiscence. Testing this hypothesis will require the identification of the transporter(s) responsible for potassium accumulation in the anthers, and their analysis in *AhZIP6-1* plants. It may also be interesting to measure potassium content in other indehiscent anther mutants (Kim et al., 2010; Sanders et al., 1999).

Ionome profiling of *AhZIP6-1* indehiscent anthers also revealed a magnesium accumulation (Figure 5a). Proper magnesium homeostasis has been linked to plant reproduction, especially to pollen development (Chen et al., 2009; Dhaka et al., 2020; Li et al., 2008; Mueller-Roeber & Arvidsson, 2009; Xu et al., 2015). For instance, the magnesium transporter MGT5 is important for tapetum function (Xu et al., 2015). In *AhZIP6-1* plants, the *MHX* gene (Figure 5e), encoding a zinc and magnesium vacuolar transporter (Shaul et al., 1999), was induced in stamens, which may account for magnesium accumulation there (Figure 5a). The higher expression of *MHX* in *AhZIP6-1* stamens may compensate the zinc homeostasis perturbation due to the higher expression of *ZIP6*, as found in *A. halleri*. Indeed, the MHX protein levels are higher in *A. halleri* shoots compared to *A. thaliana* (Elbaz et al., 2006), and this may counterbalance the higher *ZIP6* expression in *A. halleri*.

Although, at an organ level, zinc concentration was not altered in anthers of *AhZIP6-1* lines (Figure 5c), we observed that the male sterility could be rescued by the expression of *AhHMA4* in these lines, suggesting that anther indehiscence primarily resulted from altered zinc distribution in anther cells or tissues (Figure 6a). As the HMA4 and ZIP6 proteins are driving zinc transport in opposite directions, out of the cytoplasm for HMA4 and to the cytoplasm for ZIP6 (Guerinot, 2000; Hanikenne et al., 2008; Hussain et al., 2004; Talke et al., 2006; Williams & Mills, 2005), at a cellular level, HMA4 expression likely counterbalances the deleterious action of ZIP6 in *A. thaliana* stamens (Figure 6a). Increased magnesium and potassium levels, and the consecutive anther indehiscence phenotype, would thus result from processes (e.g., high *MHX* expression) compensating altered zinc homeostasis in *AhZIP6-1* lines. Several zinc finger proteins were identified to be involved in tapetum degeneration (Kapoor et al., 2002; Zhang et al., 2008). Altered zinc homeostasis may affect the function of these proteins and lead to the developmental defects observed in *AhZIP6-1* anthers (Figure 4). Many metal homeostasis mutants (e.g., *frd3*, *hma2hma4*, *nas4x-2* or *ysl1ysl3*) display altered anther and/or pollen development, which has been linked to zinc and/or iron deficiency in flowers (Hermand et al., 2014; Hussain et al., 2004; Roschzttardtz et al., 2011; Schuler, Rellán-Álvarez, Fink-Straube, Abadia, & Bauer, 2012; Waters et al., 2006), highlighting the importance of proper metal homeostasis for male fertility.

The expression patterns of *AhZIP6-1* and *AhZIP6-2* in stamens of *A. thaliana* and *A. halleri* were very similar (Figure 4 and Figure S3), suggesting conserved *cis* regulation as in root and shoot tissues (Spielmann et al., 2020). In both species, *AhZIP6-1* was highly expressed in stamen connective and, in contrast, *AhZIP6-2* expression, as evidenced by GUS staining, was not detectable. However, *AhZIP6-1* expression triggers male sterility in *A. thaliana* and not in *A. halleri*. We hypothesize that in *A. halleri*, the undesirable effects of *AhZIP6* in stamens are compensated by *AhHMA4*, which has an expression profile very similar to *AhZIP6-1* in stamens (Figures 4 and 6) and is constitutively overexpressed in *A. halleri* (Hanikenne et al., 2008). This mechanism is therefore reconstituted in *AhZIP6-1*/*AhHMA4* double homozygous lines in *A. thaliana* as discussed above. This suggests that a fine balance among overexpressed zinc transporter genes is required in *A. halleri* to enable zinc hyperaccumulation while maintaining key developmental processes such as reproduction.

In summary, in this study, the different overexpression levels of *AhZIP6-1* and *AhZIP6-2* in *A. thaliana*, without ectopic pattern – their expression pattern is similar to the endogenous *AtZIP6* –, allowed to shed light on the link between zinc and fertility. Our data highlight the need for optimal zinc homeostasis for stamen development and pollen release. Moreover, although it only moderately affects the ionome of the plants, as previously reported (Spielmann et al., 2020), the presented data support the working hypothesis that *AhZIP6* is key to fine-tune metal distribution at local scale, controlling metal homeostasis in specific cell-types (Spielmann et al., 2020). Finally, this study illustrates how the characterization of metal hyperaccumulation mechanisms can reveal key nodes and processes in the metal homeostasis network.

4 | METHODS

4.1 | Plant material, growth conditions and transformation

Arabidopsis thaliana (accession Columbia-0, Col-0) and *A. halleri* ssp. *halleri* (accession Langelsheim) were used for all experiments. The

AhZIP6-1, *AhZIP6-2*, *AhHMA4* lines represent Col-0 plants expressing *AhZIP6* under the control of the pAhZIP6-1 and pAhZIP6-2 promoters (Spielmann et al., 2020) or *AhHMA4* under the control of the pAhHMA4-2 promoter (Nouet et al., 2015), respectively. Note that the two *AhZIP6* copies mostly differ in promoter sequences and have almost identical coding sequences (Spielmann et al., 2020). The pAhZIP6-1::GUS, and pAhZIP6-2::GUS lines in *A. thaliana* or *A. halleri* were previously described (Spielmann et al., 2020), and pAhHMA4-2::GUS *A. thaliana* lines are Col-0 expressing the construct described in the 'Cloning and DNA manipulation' section below. Seeds were surface-sterilized using chloral vapor, and sown on solid agar (0.8% w/v; Select Agar; Sigma Aldrich) ½ MS medium (Duchefa Biochimie) supplemented with sucrose (1% w/v; Duchefa Biochimie) and placed at 4°C for 2 days (*A. thaliana*) or 2 weeks (*A. halleri*). Two weeks after germination, *A. thaliana* seedlings were transferred on soil or in hydroponic trays (Araponics). For hydroponic experiments, plants were grown for 3 weeks in control Hoagland medium, then submitted to experimental conditions until silique development. The nutrient solution was exchanged with a fresh medium once a week. The control Hoagland medium was modified as in (Hanikenne et al., 2008; Talke et al., 2006) and included 1 μM zinc ($ZnSO_4.H_2O$) and 10 μM FeIII-HBED [*N*,*N*′-di (2-hydroxybenzyl) ethylenediamine *N*,*N*′-diacetic acid monohydrochloride]. Zinc was omitted from the medium for deficiency experiments and 10 μM or 20 μM zinc were added for a weak or strong excess, respectively. Plants were cultivated in climate-controlled growth chambers at 20°C (night and day), with either a photoperiod of 8 hr (short days, for vegetative *A. thaliana* experiments) or 16 hr (long days, for *A. thaliana* flowering experiments) light (100 μmol photon m^{-2} s^{-1}). To obtain flowers of *A. halleri*, plants propagated by cutting were cultivated a couple of months at 20°C (long days), then cold-treated (at least 8 weeks at 4°C, short days) and placed back to 20°C (long days) until flowering. Details on experimental replication are provided in figure legends.

4.2 | T-DNA mapping and plant genotyping

As homozygous *AhZIP6-1 A. thaliana* lines were male sterile, phenotyping experiments were performed by selecting vegetative homozygous plants from segregating populations. This required prior identification of homozygous plants by genotyping. To achieve this, the insertion sites of pAhZIP6-1::*AhZIP6* T-DNA in the genome of three independent lines were first mapped using a HiTAIL-PCR approach as described (Liu & Chen, 2007). Two successive PCR were required: (a) a degenerated primer (5′-acgatggactccagagcggccgcvnvnnnggaa-3′) was combined to a T-DNA specific primer (5′-ttcccagataagggaattagggttc-3′) for a first PCR and (b) a primer (5′-acgatggactccagag-3′) specific to the degenerate primer was combined to a second T-DNA specific primer (5′-acgatggactccagtccggccgtttcgctcatgtgttgagcatataag-3′) in a second PCR. The amplified segments were cloned into the pJET1.2/blunt cloning vector (ThermoFischer Scientific), sequenced and mapped to the *A. thaliana* genome to identify the T-DNA insertion site. Based on this, three primers were designed for genotyping each line: (a) a forward primer upstream of the insertion site (primer A), (b) a reverse primer downstream of the insertion site (primer B) and (c) a reverse primer specific of the T-DNA (primer C) (Table S1). Two PCRs were performed on genomic DNA of each plant and plants with a negative first PCR (primer A + B) and a second positive PCR (primer B + C) were determined as homozygote for *AhZIP6-1*.

4.3 | Measurement of silique length and seed counting

Silique length was measured using a ruler. The same siliques were then discoloured by two successive 48 hr of incubation in 70% ethanol. The number of seeds per silique was then counted using a Nikon SMZ1500 binocular.

4.4 | Crosses and segregation analysis

As their pollen was not released, homozygote *AhZIP6-1 A. thaliana* plants were always used as mother plants in crosses. Pollen was from heterozygote and homozygote *AhZIP6-1*, homozygous pAhHMA4-2::AhHMA4 or Col-0 plants. For segregation analysis, seeds from heterozygote *AhZIP6*-1 plants (three independent lines) were germinated on ½ MS agar medium with 1% sucrose and antibiotic selection (kanamycine, 50 μg/ml, Duchefa Biochemie). Seedling were genotyped as described above by PCR. Pollen fertility was determined by silique phenotypical analysis of the F1 plants of crosses between heterozygote and homozygote *AhZIP6-1* plants.

4.5 | Histochemical staining

GUS staining was performed as described (Jefferson, Kavanagh, & Bevan, 1987). Samples were incubated between 30 min and 24 hr in staining solution. Tissues were then fixed and discoloured as described (Hanikenne et al., 2008).

Lugol staining was performed on pollen grains. Stamens were manually opened using tweezers. Pollen grains were then placed on microscope slide by strumming stamen and a drop of 100% lugol was added. After a 2 min incubation at room temperature, pictures were taken using a Nikon SMZ1500 binocular.

For Alexander staining, yellow but not yet opened stamens [anther development stage 11 or 12 according to Sanders et al., 1999 and flower development stage 12 according to Alvarez-Buylla et al., 2010] were placed in Alexander staining solution (Alexander, 1969) and incubated 5 hr at 50°C. Stamens were then washed with distilled water. Stained stamens were placed between microscope slide and lamella, and stamens were opened by gentle circular squashing. Pictures were taken using a Nikon SMZ1500 binocular.

4.6 | Pollen germination assay

Pollen grains and stamens were deposited on a pollen germination medium as described (Boavida & McCormick, 2007; Johnson-Brousseau & McCormick, 2004) and the plates were incubated 24 hr at 25°C in a high humidity environment. Pictures were then taken with a Nikon SMZ1500 binocular.

4.7 | Root and floral stem grafting

Root grafting were inspired by Turnbull, Booker, and Leyser (2002). A sterile glass microscope slide was placed on a solid ½ MS + 1% sucrose plate. On this slide, seedlings with two- to three-centimetre-long roots were placed with the root in contact with the medium whereas hypocotyls and cotyledons were in contact with the glass slide to prevent the development of adventitious roots. Both cotyledons were removed using a scalpel and hypocotyls were horizontally cut in their middle. Shoots were moved to their new roots and closely joined. After a 1 week of growth, adventitious roots were cut using a scalpel. The plants were then transferred on soil and grown until flowering. Floral stem grafting was performed as described in Nisar, Verma, Pogson, and Cazzonelli (2012).

4.8 | Gene expression analyses

Total RNA was extracted from plant tissues (100 mg for inflorescences, 20 flowers or around 800 stamens) using the NucleoSpin® RNA Plant Kit (Macherey-Nagel). cDNAs were synthesized with the RevertAid H Minus First Strand cDNA Synthesis Kit (ThermoFisher Scientific) using Oligo(dT) and 1 μg of total RNAs. cDNA were 50-fold diluted and quantitative PCR, quality control and primer efficiency correction were done as described (Spielmann et al., 2020). Relative transcript level normalization was performed using At1g58050 and *EF1a* (Nouet et al., 2015). Primer sequences are provided in Table S2.

4.9 | Cloning and DNA manipulation

The pAhHMA4-2::AhHMA4 construct was described in Nouet et al. (2015). The pAhHMA4-2::GUS was obtained by extending in 5′ the short pAhHMA4-2 fragment (1,281 bp) described in Hanikenne et al. (2008) with a 982 bp fragment from the longer pAhHMA4-2 promoter described in Nouet et al. (2015).

4.10 | Histological sections

Samples were fixed overnight in FAA (37% Formaldehyde: Ethanol: Acetic Acid, 2:17:1 v:v) at 4°C. After dehydration in a graded ethanol series, samples were cleared in Histo-Clear, embedded in paraffin and sectioned at 5 μm with a microtome. For Toluidine Blue staining, sections were stained in aqueous 0.2% Toluidine Blue for 1 min before rinsing and mounting in Entellan (Merck 107,961). For Phloroglucinol staining, sections were incubated 1 hr at room temperature in a 2% (w/v) Phloroglucinol in 100% EtOh. Then, sections were mounted with 18.5% (v/v) HCl.

4.11 | Analysis of metal contents

Stamens (100/sample) were digested with 3 ml of ≥65% HNO_3 (Sigma-Aldrich) using a DigiPrep Graphite Block Digestion System (SCP Science) as follows: 10 min at 45°C, 10 min at 65°C and 90 min at 105°C. Once cooled, sample volumes were adjusted with distilled water to 50 ml and samples were analysed by inductively coupled plasma-mass spectrometry (ICP-MS) (ELAN DRC II, Perkin Elmer SCIEX).

Flowers (5 mg of dry flowers/sample) were acid-digested as described above. Once cooled, sample volumes were adjusted to 10 ml with distilled water and 200 μl of ≥65% HNO_3 (Sigma-Aldrich) were added. Metal concentrations were determined using inductively coupled plasma atomic emission spectroscopy (ICP-AES) with a Vista-AX instrument (Varian, Melbourne, Australia).

4.12 | Yeast tolerance and complementation assays

The CM66 yeast strain (*alr1alr2*) (Li et al., 2001) and the corresponding parental strain CM52 were transformed with an empty pFL38 vector and/or a pFL38 vector expressing *AhZIP6* under the control of promoter pGK1 (Spielmann et al., 2020). Transformants were selected on SC-Leu medium (MP Biomedicals) containing 250 mM magnesium to allow the growth of CM66. For each genotype, three independent colonies were grown in 2 ml liquid medium SC-Leu (MP Biomedicals) for 2 days at 30°C with a 250 rpm agitation. Five hundred microliters of the cultures were then harvested by centrifugation and resuspended in water. For drop tests, the yeast suspension was serially diluted to OD_{600} of 0.2, 0.02, 0.002 and 10 μl of each serial dilution was dropped on SC-Leu (MP Biomedicals) plates containing 4 or 250 mM of $MgS0_4$ and observations were made after 4 days of growth at 30°C.

ACKNOWLEDGMENTS

We thank Prof. N. Verbruggen, Prof. S. Clemens and Dr. S. Fanara for helpful discussions, as well as V. Deblander, V. Crutzen and M. Scheepers for technical assistance. *A. thaliana HMA4*-expressing lines were provided by Dr. C. Nouet. We thank Prof. S. Gobert and R. Biondi for ICP-MS analysis. We thank Prof. R. Gardner for the kind gift of the CM66 and CM52 yeast strains. Funding was provided by the 'Fonds de la Recherche Scientifique–FNRS' (PDR-T.0206.13, MIS-F.4511.16, CDR J.0009.17, PDR T0120.18) (Marc Hanikenne), the University of Liège (SFRD-12/03) (Marc Hanikenne) and the Belgian Program on Interuniversity Attraction Poles (IAP no. P7/44) (Marc Hanikenne). Marc Hanikenne was Senior Research Associate of the F.R.S.-FNRS. Julien Spielmann was doctoral fellow of the FNRS.

CONFLICT OF INTEREST

No conflict of interest declared.

DATA AVAILABILITY STATEMENT

The data that support the findings of this study are available from the corresponding author upon reasonable request.

ORCID

Julien Spielmann https://orcid.org/0000-0003-1327-3975
Noémie Thiébaut https://orcid.org/0000-0001-8075-1303
Claire Périlleux https://orcid.org/0000-0001-7653-2431
Marc Hanikenne https://orcid.org/0000-0002-8964-9601

REFERENCES

Ahmadi, H., Corso, M., Weber, M., Verbruggen, N., & Clemens, S. (2018). CAX1 suppresses Cd-induced generation of reactive oxygen species in *Arabidopsis halleri*. *Plant, Cell and Environment*, *41*, 2435–2448.

Albrecht, C., Russinova, E., Hecht, V., Baaijens, E., & de Vries, S. (2005). The Arabidopsis thaliana SOMATIC EMBRYOGENESIS RECEPTOR-LIKE KINASES1 and 2 control male sporogenesis. *The Plant Cell*, *17*, 3337–3349.

Alexander, M. P. (1969). Differential staining of aborted and nonaborted pollen. *Stain Technology*, *44*, 117–122.

Alvarez-Buylla, E., Benítez, M., Corvera-Poiré, A., Chaos Cador, Á., de Folter, S., Gamboa de Buen, A., … Sánchez-Corralesa, Y. (2010). Flower development. In *The Arabidopsis book*. Washington, DC: BioOne. https://doi.org/10.1199/tab.0127

Bassil, E., Tajima, H., Liang, Y. C., Ohto, M. A., Ushijima, K., Nakano, R., … Blumwald, E. (2011). The *Arabidopsis* Na+/H+ antiporters NHX1 and NHX2 control vacuolar pH and K+ homeostasis to regulate growth, flower development, and reproduction. *The Plant Cell*, *23*, 3482–3497.

Boavida, L. C., & McCormick, S. (2007). Temperature as a determinant factor for increased and reproducible in vitro pollen germination in *Arabidopsis thaliana*. *Plant Journal*, *52*, 570–582.

Bock, K. W., Honys, D., Ward, J. M., Padmanaban, S., Nawrocki, E. P., Hirschi, K. D., … Sze, H. (2006). Integrating membrane transport with male gametophyte development and function through transcriptomics. *Plant Physiology*, *140*, 1151–1168.

Brown, D. M., Zeef, L. A., Ellis, J., Goodacre, R., & Turner, S. R. (2005). Identification of novel genes in Arabidopsis involved in secondary cell wall formation using expression profiling and reverse genetics. *The Plant Cell*, *17*, 2281–2295.

Chen, J., Li, L. G., Liu, Z. H., Yuan, Y. J., Guo, L. L., Mao, D. D., … Li, D. P. (2009). Magnesium transporter AtMGT9 is essential for pollen development in *Arabidopsis*. *Cell Research*, *19*, 887–898.

Colcombet, J., Boisson-Dernier, A., Ros-Palau, R., Vera, C. E., & Schroeder, J. I. (2005). Arabidopsis SOMATIC EMBRYOGENESIS RECEPTOR KINASES1 and 2 are essential for tapetum development and microspore maturation. *The Plant Cell*, *17*, 3350–3361.

Curie, C., Cassin, G., Couch, D., Divol, F., Higuchi, K., Le Jean, M., … Mari, S. (2009). Metal movement within the plant: Contribution of nicotianamine and yellow stripe 1-like transporters. *Annals of Botany*, *103*, 1–11.

D'Ippolito, S., Arias, L. A., Casalongue, C. A., Pagnussat, G. C., & Fiol, D. F. (2017). The DC1-domain protein VACUOLELESS GAMETOPHYTES is essential for development of female and male gametophytes in Arabidopsis. *Plant Journal*, *90*, 261–275.

Dawson, J., Zen, E., Vizir, I., Van Waeyenberge, S., Wilson, Z., & Mulligan, B. (1999). Characterization and genetic mapping of a mutation (*ms35*) which prevents anther dehiscence in *Arabidopsis thaliana* by affecting secondary wall thickening in the endothecium. *New Phytologist*, *144*, 213–222.

Deinlein, U., Weber, M., Schmidt, H., Rensch, S., Trampczynska, A., Hansen, T. H., … Clemens, S. (2012). Elevated nicotianamine levels in *Arabidopsis halleri* roots play a key role in zinc hyperaccumulation. *The Plant Cell*, *24*, 708–723.

Dhaka, N., Krishnan, K., Kandpal, M., Vashisht, I., Pal, M., Sharma, M. K., & Sharma, R. (2020). Transcriptional trajectories of anther development provide candidates for engineering male fertility in sorghum. *Scientific Reports*, *10*, 897.

Elbaz, B., Shoshani-Knaani, N. O. A., David-Assael, O. R. A., Mizrachy-Dagri, T., Mizrahi, K., Saul, H., … Shaul, O. (2006). High expression in leaves of the zinc hyperaccumulator *Arabidopsis halleri* of *AhMHX*, a homolog of an *Arabidopsis thaliana* vacuolar metal/proton exchanger. *Plant, Cell and Environment*, *29*, 1179–1190.

Gomez, J. F., Talle, B., & Wilson, Z. A. (2015). Anther and pollen development: A conserved developmental pathway. *Journal of Integrative Plant Biology*, *57*, 876–891.

Guerinot, M. L. (2000). The ZIP family of metal transporters. *Biochimica et Biophysica Acta*, *1465*, 190–198.

Hanikenne, M., Esteves, S. M., Fanara, S., & Rouached, H. (2021). Coordinated homeostasis of essential mineral nutrients: A focus on iron. *Journal of Experimental Botany*, *72*, 2136–2153.

Hanikenne, M., & Nouet, C. (2011). Metal hyperaccumulation and hypertolerance: A model for plant evolutionary genomics. *Current Opinion in Plant Biology*, *14*, 252–259.

Hanikenne, M., Talke, I. N., Haydon, M. J., Lanz, C., Nolte, A., Motte, P., … Krämer, U. (2008). Evolution of metal hyperaccumulation required *cis*-regulatory changes and triplication of *HMA4*. *Nature*, *453*, 391–395.

Hermand, V., Julio, E., Dorlhac de Borne, F., Punshon, T., Ricachenevsky, F. K., Bellec, A., … Berthomieu, P. (2014). Inactivation of two newly identified tobacco heavy metal ATPases leads to reduced Zn and Cd accumulation in shoots and reduced pollen germination. *Metallomics: Integrated Biometal Science*, *6*, 1427–1440.

Hussain, D., Haydon, M. J., Wang, Y., Wong, E., Sherson, S. M., Young, J., … Cobbett, C. S. (2004). P-type ATPase heavy metal transporters with roles in essential zinc homeostasis in Arabidopsis. *The Plant Cell*, *16*, 1327–1339.

Jakobsen, M., Poulsen, L., Schulz, A., Fleurat-Lessard, P., Møller, A., Husted, S., … Palmgren, M. (2005). Pollen development and fertilization in *Arabidopsis* is dependent on the *MALE GAMETOGENESIS IMPAIRED ANTHERS* gene encoding a type V P-type ATPase. *Genes and Development*, *19*, 2757–2769.

Jefferson, R. A. K., Kavanagh, T. A., & Bevan, M. W. (1987). GUS fusions: β-glucuronidase as a sensitive and versatile gene fusion marker in higher plants. *EMBO Journal*, *6*, 3901–3907.

Jochner, S., Hofler, J., Beck, I., Gottlein, A., Ankerst, D. P., Traidl-Hoffmann, C., & Menzel, A. (2013). Nutrient status: A missing factor in phenological and pollen research? *Journal of Experimental Botany*, *64*, 2081–2092.

Johnson-Brousseau, S. A., & McCormick, S. (2004). A compendium of methods useful for characterizing *Arabidopsis* pollen mutants and gametophytically-expressed genes. *Plant Journal*, *39*, 761–775.

Jung, K. W., Oh, S. I., Kim, Y. Y., Yoo, K. S., Cui, M. H., & Shin, J. S. (2008). Arabidopsis Histidine-containing Phosphotransfer factor 4 (AHP4) negatively regulates secondary wall thickening of the anther endothecium during flowering. *Molecules and Cells*, *25*, 294–300.

Kapoor, S., Kobayashi, A., & Takatsuji, H. (2002). Silencing of the Tapetum-specific zinc finger gene TAZ1 causes premature degeneration of Tapetum and pollen abortion in petunia. *The Plant Cell*, *14*, 2353–2367.

Keijzer, C. J. (1987). The processes of anther dehiscence and pollen dispersal. I. the opening mechanism of longitudinally dehiscing anthers. *New Phytologist*, *105*, 487–498.

Kim, S. G., Lee, S., Kim, Y. S., Yun, D. J., Woo, J. C., & Park, C. M. (2010). Activation tagging of an Arabidopsis SHI-RELATED SEQUENCE gene produces abnormal anther dehiscence and floral development. *Plant Molecular Biology*, *74*, 337–351.

Kim, Y. Y., Jung, K. W., Jeung, J. U., & Shin, J. S. (2012). A novel F-box protein represses endothecial secondary wall thickening for anther dehiscence in Arabidopsis thaliana. *Journal of Plant Physiology*, *169*, 212–216.

Krämer, U. (2010). Metal hyperaccumulation in plants. *Annual Review of Plant Biology*, *61*, 517–534.

Krämer, U., Talke, I. N., & Hanikenne, M. (2007). Transition metal transport. *FEBS Letters*, *581*, 2263–2272.

Li, L., Tutone, A. F., Drummond, R. S., Gardner, R. C., & Luan, S. (2001). A novel family of magnesium transport genes in Arabidopsis. *The Plant Cell*, *13*, 2761–2775.

Li, L. G., Sokolov, L. N., Yang, Y. H., Li, D. P., Ting, J., Pandy, G. K., & Luan, S. (2008). A mitochondrial magnesium transporter functions in *Arabidopsis* pollen development. *Molecular Plant*, *1*, 675–685.

Liu, Y. G., & Chen, Y. (2007). High-efficiency thermal asymmetric interlaced PCR for amplification of unknown flanking sequences. *BioTechniques*, *43*, 649–654.

Matsui, T., Omasa, K., & Horie, T. (2000). Rapid swelling of pollen grains in the dehiscing anther of two-rowed barley (Hordeum distichum L. emend. LAM.). *Annals of Botany*, *85*, 345–350.

Merlot, S., de la Torre, V. S. G., & Hanikenne, M. (2021). Physiology and molecular biology of trace element Hyperaccumulation. In A. van der Ent, A. J. M. Baker, G. Echevarria, M-O. Simonnot, & J. L. Morel (Eds.), *Agromining: Farming for Metals - Extracting Unconventional Resources Using Plants (2d edition)* (pp. 93–116). Springer Nature Switzerland AG.

Mitsuda, N., Iwase, A., Yamamoto, H., Yoshida, M., Seki, M., Shinozaki, K., & Ohme-Takagi, M. (2007). NAC transcription factors, NST1 and NST3, are key regulators of the formation of secondary walls in woody tissues of Arabidopsis. *The Plant Cell*, *19*, 270–280.

Mitsuda, N., Seki, M., Shinozaki, K., & Ohme-Takagi, M. (2005). The NAC transcription factors NST1 and NST2 of Arabidopsis regulate secondary wall thickenings and are required for anther dehiscence. *The Plant Cell*, *17*, 2993–3006.

Mueller-Roeber, B., & Arvidsson, S. (2009). Fertility control: The role of magnesium transporters in pollen development. *Cell Research*, *19*, 800–801.

Nisar, N., Verma, S., Pogson, B. J., & Cazzonelli, C. I. (2012). Inflorescence stem grafting made easy in Arabidopsis. *Plant Methods*, *8*, 50.

Nouet, C., Charlier, J.-B., Carnol, M., Bosman, B., Farnir, F., Motte, P., & Hanikenne, M. (2015). Functional analysis of the three *HMA4* copies of the metal hyperaccumulator *Arabidopsis halleri*. *Journal of Experimental Botany*, *66*, 5783–5795.

Olsen, L. I., Hansen, T. H., Larue, C., Østerberg, J. T., Hoffmann, R. D., Liesche, J., … Palmgren, M. (2016). Mother-plant-mediated pumping of zinc into the developing seed. *Nature Plants*, *2*, 16036.

Olsen, L. I., & Palmgren, M. G. (2014). Many rivers to cross: The journey of zinc from soil to seed. *Frontiers in Plant Science*, *5*, 30.

Pacini, E. (2010). Relationships between Tapetum, Loculus, and pollen during development. *International Journal of Plant Sciences*, *171*, 1–11.

Pacini, E., Franchi, G., & Hesse, M. (1985). The Tapetum its form, function, and possible phylogeny in *Embryophyta*. *Plant Systematics and Evolution*, *149*, 155–185.

Pandey, N., Pathak, G. C., & Sharma, C. P. (2006). Zinc is critically required for pollen function and fertilisation in lentil. *Journal of Trace Elements in Medicine and Biology: Organ of the Society for Minerals and Trace Elements*, *20*, 89–96.

Ravet, K., Touraine, B., Boucherez, J., Briat, J. F., Gaymard, F., & Cellier, F. (2009). Ferritins control interaction between iron homeostasis and oxidative stress in Arabidopsis. *Plant Journal*, *57*, 400–412.

Reeves, R. D., Baker, A. J., Jaffré, T., Erskine, P. D., Echevarria, G., & van der Ent, A. (2018). A global database for plants that hyperaccumulate metal and metalloid trace elements. *New Phytologist*, *218*, 407–411.

Rehman, S., & Yun, S. J. (2006). Developmental regulation of K accumulation in pollen, anthers, and papillae: Are anther dehiscence, papillae hydration, and pollen swelling leading to pollination and fertilization in barley (Hordeum vulgare L.) regulated by changes in K concentration? *Journal of Experimental Botany*, *57*, 1315–1321.

Ricachenevsky, F. K., Menguer, P. K., Sperotto, R. A., & Fett, J. P. (2015). Got to hide your Zn away: Molecular control of Zn accumulation and biotechnological applications. *Plant Science*, *236*, 1–17.

Roschzttardtz, H., Seguela-Arnaud, M., Briat, J. F., Vert, G., & Curie, C. (2011). The FRD3 citrate effluxer promotes iron nutrition between symplastically disconnected tissues throughout *Arabidopsis* development. *The Plant Cell*, *23*, 2725–2737.

Sanders, P. M., Bui, A. Q., Weterings, K., McIntire, K. N., Hsu, Y.-C., Lee, P. Y., … Goldberg, R. B. (1999). Anther developmental defects in *Arabidopsis thaliana* male-sterile mutants. *Sexual Plant Reproduction*, *11*, 297–322.

Schuler, M., Rellán-Álvarez, R., Fink-Straube, C., Abadia, J., & Bauer, P. (2012). Nicotianamine functions in the phloem-based transport of iron to sink organs, in pollen development and pollen tube growth in *Arabidopsis*. *The Plant Cell*, *24*, 2380–2400.

Scott, R. J., Spielman, M., & Dickinson, H. G. (2004). Stamen structure and function. *The Plant Cell*, *16*, S46–S60.

Shaul, O., Hilgemann, D. W., De-Almeida-Engler, J., van Montagu, M., Inzé, D., & Galili, G. (1999). Cloning and characterization of a novel Mg^{2+}/H^{+} exchanger. *EMBO Journal*, *18*, 3973–3980.

Sinclair, S. A., & Krämer, U. (2012). The zinc homeostasis network of land plants. *Biochimica et Biophysica Acta*, *1823*, 1553–1567.

Spielmann, J., Ahmadi, H., Scheepers, M., Weber, M., Nitsche, S., Carnol, M., … Hanikenne, M. (2020). The two copies of the zinc and cadmium ZIP6 transporter of Arabidopsis halleri have distinct effects on cadmium tolerance. *Plant, Cell & Environment*, *43*, 2143–2157.

Spielmann, J., & Vert, G. (2021). The many facets of protein ubiquitination and degradation in plant root iron deficiency responses. *Journal of Experimental Botany*, *72*, 2071–2082.

Stacey, M. G., Koh, S., Becker, J., & Stacey, G. (2002). AtOPT3, a member of the oligopeptide transporter family, is essential for embryo development in Arabidopsis. *The Plant Cell*, *14*, 2799–2811.

Stacey, M. G., Patel, A., McClain, W. E., Mathieu, M., Remley, M., Rogers, E. E., … Stacey, G. (2008). The Arabidopsis AtOPT3 protein functions in metal homeostasis and movement of iron to developing seeds. *Plant Physiology*, *146*, 589–601.

Steiner-Lange, S., Unte, U., Eckstein, L., Yang, C., Wilson, Z., Schmelzer, E., … Saedler, H. (2003). Disruption of Arabidopsis thaliana *MYB26* results in male sterility due to non-dehiscent anthers. *Plant Journal*, *34*, 519–528.

Talke, I. N., Hanikenne, M., & Krämer, U. (2006). Zinc-dependent global transcriptional control, transcriptional deregulation, and higher gene copy number for genes in metal homeostasis of the hyperaccumulator *Arabidopsis halleri*. *Plant Physiology*, *142*, 148–167.

Turnbull, C. G., Booker, J. P., & Leyser, H. M. (2002). Micrografting techniques for testing long-distance signalling in *Arabidopsis*. *Plant Journal*, *32*, 255–262.

van der Ent, A., Baker, A. J., Reeves, R. D., Pollard, A. J., & Schat, H. (2013). Hyperaccumulators of metal and metalloid trace elements: Facts and fiction. *Plant and Soil*, *362*, 319–334.

Villarreal, F., Martin, V., Colaneri, A., Gonzalez-Schain, N., Perales, M., Martin, M., … Zabaleta, E. (2009). Ectopic expression of mitochondrial gamma carbonic anhydrase 2 causes male sterility by anther indehiscence. *Plant Molecular Biology*, *70*, 471–485.

Walker, E. L., & Waters, B. M. (2011). The role of transition metal homeostasis in plant seed development. *Current Opinion in Plant Biology*, *14*, 318–324.

Waters, B. M., Chu, H. H., Didonato, R. J., Roberts, L. A., Eisley, R. B., Lahner, B., … Walker, E. L. (2006). Mutations in Arabidopsis *yellow stripe-like1* and *yellow stripe-like3* reveal their roles in metal ion

homeostasis and loading of metal ions in seeds. *Plant Physiology*, *141*, 1446–1458.

Wei, D., Liu, M., Chen, H., Zheng, Y., Liu, Y., Wang, X., … Lin, J. (2018). INDUCER OF CBF EXPRESSION 1 is a male fertility regulator impacting anther dehydration in *Arabidopsis*. *PLoS Genetics*, *14*, e1007695.

Williams, L. E., & Mills, R. F. (2005). P_{1B}-ATPases-an ancient family of transition metal pumps with diverse functions in plants. *Trends in Plant Science*, *10*, 491–502.

Wilson, Z. A., Song, J., Taylor, B., & Yang, C. (2011). The final split: The regulation of anther dehiscence. *Journal of Experimental Botany*, *62*, 1633–1649.

Xu, L., Xiong, X., Liu, W., Liu, T., Yu, Y., & Cao, J. (2020). BcMF30a and BcMF30c, two novel non-tandem CCCH zinc-finger proteins, function in pollen development and pollen germination in Brassica campestris ssp. chinensis. *International Journal of Molecular Sciences*, *21*, 6428.

Xu, X. F., Wang, B., Lou, Y., Han, W. J., Lu, J. Y., Li, D. D., … Yang, Z. N. (2015). *Magnesium transporter 5* plays an important role in mg transport for male gametophyte development in *Arabidopsis*. *Plant Journal*, *84*, 925–936.

Yan, J., Chia, J. C., Sheng, H., Jung, H. I., Zavodna, T. O., Zhang, L., … Vatamaniuk, O. K. (2017). Arabidopsis pollen fertility requires the transcription factors CITF1 and SPL7 that regulate copper delivery to anthers and Jasmonic acid synthesis. *The Plant Cell*, *29*, 3012–3029.

Yang, C., Vizcay-Barrena, G., Conner, K., & Wilson, Z. A. (2007). MALE STERILITY1 is required for tapetal development and pollen wall biosynthesis. *The Plant Cell*, *19*, 3530–3548.

Yang, C., Xu, Z., Song, J., Conner, K., Vizcay Barrena, G., & Wilson, Z. A. (2007). Arabidopsis MYB26/MALE STERILE35 regulates secondary thickening in the endothecium and is essential for anther dehiscence. *The Plant Cell*, *19*, 534–548.

Yang, S. L., Xie, L. F., Mao, H. Z., Puah, C. S., Yang, W. C., Jiang, L., … Ye, D. (2003). Tapetum determinant1 is required for cell specialization in the Arabidopsis anther. *The Plant Cell*, *15*, 2792–2804.

Zhang, D. S., Liang, W. Q., Yuan, Z., Li, N., Shi, J., Wang, J., … Zhang, D. B. (2008). Tapetum degeneration retardation is critical for aliphatic metabolism and gene regulation during rice pollen development. *Molecular Plant*, *1*, 599–610.

Zhu, J., Chen, H., Li, H., Gao, J. F., Jiang, H., Wang, C., … Yang, Z. N. (2008). Defective in Tapetal development and function 1 is essential for anther development and tapetal function for microspore maturation in Arabidopsis. *Plant Journal*, *55*, 266–277.

SUPPORTING INFORMATION

Additional supporting information may be found in the online version of the article at the publisher's website.

How to cite this article: Spielmann, J., Detry, N., Thiébaut, N., Jadoul, A., Schloesser, M., Motte, P., Périlleux, C., & Hanikenne, M. (2021). *ZRT-IRT-Like PROTEIN 6* expression perturbs local ion homeostasis in flowers and leads to anther indehiscence and male sterility. *Plant, Cell & Environment*, 1–14. https://doi.org/10.1111/pce.14200